Protein Science (1992), *1*, 761-776. Cambridge University Press. Printed in the USA.

Multiple alanine replacements within α-helix 126-134 of T4 lysozyme have independent, additive effects on both structure and stability

X.-J. ZHANG, W.A. BAASE, AND B.W. MATTHEWS

Institute of Molecular Biology, Howard Hughes Medical Institute, and
Department of Physics, University of Oregon, Eugene, Oregon 97403

(RECEIVED November 18, 1991; REVISED MANUSCRIPT RECEIVED January 30, 1992)

Abstract

In a systematic attempt to identify residues important in the folding and stability of T4 lysozyme, five amino acids within α-helix 126-134 were substituted by alanine, either singly or in selected combinations. Together with three alanines already present in the wild-type structure this provided a set of mutant proteins with up to eight alanines in sequence. All the variants behaved normally, suggesting that the majority of residues in the α-helix are nonessential for the folding of T4 lysozyme. Of the five individual alanine substitutions it is inferred that four result in slightly increased protein stability and one, the replacement of a buried leucine with alanine, substantially decreased stability. The results support the idea that alanine is a residue of high helix propensity. The change in protein stability observed for each of the multiple mutants is approximately equal to the sum of the energies associated with each of the constituent substitutions.

All of the variants could be crystallized isomorphously with wild-type lysozyme, and, with one trivial exception, their structures were determined at high resolution. Substitution of the largely solvent-exposed residues Asp 127, Glu 128, and Val 131 with alanine caused essentially no change in structure except at the immediate site of replacement. Substitutions of the partially buried Asn 132 and the buried Leu 133 with alanine were associated with modest (≤0.4 Å) structural adjustments. The structural changes seen in the multiple mutants were essentially a combination of those seen in the constituent single replacements. The different replacements therefore act essentially independently not only so far as changes in energy are concerned but also in their effect on structure. The destabilizing replacement Leu 133 → Ala made α-helix 126-134 somewhat less regular. Incorporation of additional alanine replacements tended to make the helix more uniform. For the penta-alanine variant a distinct change occurred in a crystal-packing contact, and the "hinge-bending angle" between the amino- and carboxy-terminal domains changed by 3.6°. This tends to confirm that such hinge-bending in T4 lysozyme is a low-energy conformational change.

Keywords: alanine; lysozyme; protein folding; protein structure; thermostability

In a systematic attempt to identify residues important in the folding and stability of phage T4 lysozyme we previously substituted four alanines within the α-helix that includes residues 126-134 (Zhang et al., 1991). The helix is amphipathic, located on the surface of the carboxy-terminal domain, and is remote from the active site (Fig. 1; Kinemage 1). In wild-type lysozyme this α-helix already includes three alanines. It was found that substitution of three solvent-exposed residues, Glu 128, Val 131, and Asn 132, with alanine did not interfere with folding or activity, and the multiple mutant in which all three of these residues were replaced with alanine (E128A/V131A/N132A) had a melting temperature at pH 2.0 that was 3.4 °C higher than wild type. The results therefore also supported the idea that alanine is a residue of high helix propensity (Marqusee et al., 1989; Dao-pin et al., 1990; Lyu et al., 1990; Merutka et al., 1990; O'Neil & DeGrado, 1990). It was also noted in the prior study that replacement of the buried residue Leu 133 with alanine was substantially destabilizing.

In the present report we extend these studies by including the additional substitution D127A and by con-

Reprint requests to: B.W. Matthews, Institute of Molecular Biology, Howard Hughes Medical Institute, University of Oregon, Eugene, Oregon 97403.

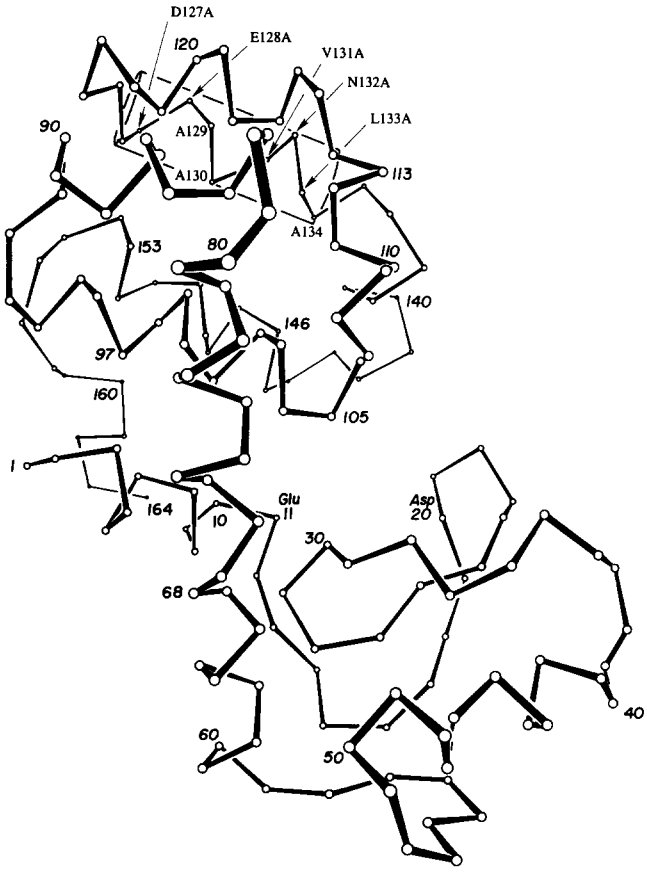

Fig. 1. Schematic drawing of the backbone structure of T4 lysozyme showing the location of the polyalanine helix and the mutations discussed in the text.

structing additional multiple mutants in which selected alanine replacements were combined in the same protein. In total, 10 different mutants have been characterized (Table 1), culminating in the variant D127A/E128A/V131A/N132A/L133A in which five substituted alanines, together with the naturally occurring ones at positions 129, 130, and 134, result in a string of eight consecutive alanines.

Results

The mutant lysozymes that are the subject of this study are summarized in Table 1. First there are three variants with single amino acid substitutions, Glu 128 → Ala (E128A), V131A, and L133A. These were then combined with two additional substitutions Asp 127 → Ala and Asn 132 → Ala to give the double mutants, D127A/E128A, E128A/V131A, and V131A/N132A. Further combinations provided the triple mutant E128A/V131A/N132A, which will be further abbreviated to 128/131/132, the quadruple mutants 127/128/131/132 and 128/131/132/133, and the quintuple mutant 127/128/131/132/133. The first quadruple variant has six alanines in sequence, from residue 127 to 132, and is also referred to as A127-132, the second quadruple variant has seven alanines in sequence (A128-134), and the quintuple mutant (A127-134) has eight consecutive alanines.

Notwithstanding the introduction of up to five additional alanines, all of the mutant lysozymes behaved normally and could be purified by the standard procedure (Muchmore et al., 1989; Poteete et al., 1991).

The stabilities of the mutant lysozymes as measured by reversible unfolding at pH 2.0 are given in Table 2. The overall result is that all mutants except those that included replacement of the buried residue Leu 133 with alanine resulted in an increase in thermostability.

All of the mutants could be crystallized using conditions similar to those for wild-type lysozyme (Weaver & Matthews, 1987) and gave crystals large enough for high-resolution data collection. Prior to X-ray exposure the crystals were equilibrated with a solution of 1.05 M K_2HPO_4, 1.26 M NaH_2PO_4, 0.23 M NaCl, 1.4 mM β-mercaptoethanol, pH 6.7. The oscillation photographic method was used to collect X-ray data for the variants L133A, E128A/V131A, V131A/N132A, and 128/131/132. A multiwire detector (San Diego Multiwire Systems) (Xuong et al., 1985) was used for the variants D127A/E128A, 128/131/132/133, 127/128/131/132, and 127/128/131/132/133. Glu 128 of T4 lysozyme is completely solvent exposed and quite mobile (average thermal factor for atoms in the carboxyl group is 77 $Å^2$). It was therefore expected that the structure of E128A would be virtually identical with that of the wild type, and no attempt was made to solve the crystal structure of the single mutant. An early study, albeit at moderate resolution, showed that the substitution Glu 128 → Lys caused very little change in the structure of T4 lysozyme (Grütter & Matthews, 1982). Verification of the minimal structural changes associated with the substitution Glu 128 → Ala is, in any event, provided by the crystal structures of E128A/V131A and other multiple mutants in which it is incorporated.

The structural changes associated with the various mutants were first visualized using difference electron density maps and then refined (Tronrud et al., 1987) using procedures essentially as described by Dao-pin et al. (1991). The refined model of wild-type lysozyme (Bell et al., 1991) was used as the starting point for refinement. In cases where the unit cell dimensions of the mutant crystal differed significantly from those of the wild type, rigid-body refinement was first used to place the whole molecule and/or the separate amino-terminal and carboxy-terminal domains within the mutant unit cell (Dao-pin et al., 1991). Data collection and refinement statistics are summarized in Table 3. Coordinates of the refined structures have been deposited in the Brookhaven Protein Data Bank.

In the following paragraphs we will briefly describe the structural changes associated with the different variants.

Table 1. *Sequences of mutant lysozymes*[a]

	α-Helix 126–134									
Lysozyme	126	127	128	129	130	131	132	133	134	135
Wild type	Trp	Asp	Glu	Ala	Ala	Val	Asn	Leu	Ala	Lys
E128A			Ala	(Ala)	(Ala)				(Ala)	
V131A				(Ala)	(Ala)	Ala			(Ala)	
L133A				(Ala)	(Ala)			Ala	(Ala)	
D127A/E128A		Ala	Ala	(Ala)	(Ala)				(Ala)	
E128A/V131A			Ala	(Ala)	(Ala)	Ala			(Ala)	
V131A/N132A				(Ala)	(Ala)	Ala	Ala		(Ala)	
E128A/V131A/N132A			Ala	(Ala)	(Ala)	Ala	Ala		(Ala)	
127/128/131/132		Ala	Ala	(Ala)	(Ala)	Ala	Ala		(Ala)	
128/131/132/133			Ala	(Ala)	(Ala)	Ala	Ala	Ala	(Ala)	
127/128/131/132/133		Ala	Ala	(Ala)	(Ala)	Ala	Ala	Ala	(Ala)	
Solvent accessibility	0.27	1.10	0.76	0.00	0.14	0.78	0.34	0.01	0.37	0.85

[a] The locations of the alanines introduced in the different mutant lysozymes are shown. Alanines in parentheses are present in both wild-type and mutant variants. The last line gives the solvent accessibility of the side chain present in the crystal structure of wild-type lysozyme. Solvent accessibility is defined as the ratio of the area of the side chain exposed to solvent in the folded structure relative to the area exposed to solvent in an extended model peptide of the same amino acid sequence.

Table 2. *Thermal stabilities of mutant lysozymes*[a]

Mutant	ΔH (kcal/mol)	ΔT_m (°C)	$\Delta\Delta G$ (kcal/mol)
Wild type[b]	86.0		
E128A[b]	85.0	0.6 ± 0.25	0.16
V131A[b]	88.7	1.0 ± 0.25	0.27
L133A	53.0	−17.0 ± 2.0	−4.19
D127A/E128A	85.8	0.9 ± 0.25	0.24
E128A/V131A[b]	93.0	1.5 ± 0.25	0.44
V131A/N132A[b]	82.0	2.3 ± 0.25	0.57
E128A/V131A/N132A[b]	88.3	3.4 ± 0.22	0.91
127/128/131/132	86.3	4.0 ± 0.25	1.01
128/131/132/133	63.9	−10.3 ± 0.5	−2.59
127/128/131/132/133	62.2	−9.4 ± 0.5	−2.27

[a] All measurements are at pH 2.02, 0.2 M KCl. ΔH is the enthalpy of unfolding at the melting temperature, T_m. ΔT_m is the difference between the melting temperature of the mutant and that of wild-type lysozyme (40.75 °C). $\Delta\Delta G$, the difference between the free energy of unfolding of the mutant and wild-type proteins, was estimated using a thermodynamic model (Brandts & Hunt, 1967; Becktel & Schellman, 1987), which includes a constant change in heat capacity, ΔC_p, estimated in this case to be 2.4 kcal/mol-deg. For the mutants whose melting temperatures are within a few degrees of wild type, the estimated error in $\Delta\Delta G$ is ±0.1 kcal/mol. For the unstable mutants, however, especially L133A, the accuracy of $\Delta\Delta G$ is limited by the choice of the model used for its determination and by the choice of ΔC_p. In addition, under the conditions used in this study (0.20 M KCl, pH 2.02), which were chosen to be consistent with the prior analysis (Zhang et al., 1991), the melting of L133A above its T_m shows some departure from two-state behavior. For these reasons the uncertainty in $\Delta\Delta G$ for L133A is difficult to estimate but could be as much as ±1 kcal/mol. Under somewhat different conditions (0.025 M potassium chloride, 0.02 M potassium phosphate, pH 3.0) (Kitamura & Sturtevant, 1989) L133A exhibits two-state melting and has an estimated $\Delta\Delta G$ of −3.6 kcal/mol (Eriksson et al., 1992).

[b] Data from Zhang et al. (1991).

Single mutant structures: L133A

D127A and N132A were not obtained as single mutants (Table 1). As explained above, the structure of E128A was not determined. The structure of V131A has been described by Dao-pin et al. (1990). This leaves L133A.

Leucine 133 is completely inaccessible to solvent. The map showing the difference in electron density between mutant and wild type (Fig. 2A) clearly indicates the loss of the leucyl side chain and also suggests some slight adjustments in neighboring parts of the structure. The refined mutant structure (Fig. 2B) indicates that the α-helical residues 109–114 move ~0.3–0.5 Å toward the space vacated by the leucyl side chain. The movement of these residues, as well as adjustments (~0.4 Å) at the substitution site itself, are also seen in a "shift plot" (Figs. 3A, 4A) showing the shift of each residue in L133A relative to wild-type lysozyme (animated in Kinemage 2). In wild-type lysozyme there is a van der Waals contact (3.6 Å) between atoms within the side chains of Leu 133 and Phe 114. In the mutant, the side chain of Phe 114 moves 0.32 Å toward the space vacated by Leu 133. Also the hydroxyl of Ser 117 moves 0.47 Å, its χ^1 angle changing from −66° to −73°. The crystallographic thermal factor of the β-carbon of Leu 133 increases from 13 Å^2 in wild type to 38 Å^2 in L133A, indicating substantially greater mobility in the latter structure.

D127A/E128A and E128A/V131A

These two variants are considered together because Asp 127, Glu 128, and Val 131 are on the solvent-exposed side

Table 3. *Data collection and refinement statistics*[a]

Mutant	133	127/128	128/131	131/132	128/131/132	127/128/ 131/132	128/131/ 132/133	127/128/ 131/132/133
Data collection								
Method	Film	Multiwire	Film	Film	Film	Multiwire	Multiwire	Multiwire
Cell dimensions								
a, b (Å)	61.3	61.1	61.2	61.2	61.3	61.4	61.4	61.1
Δa, b (Å)	0.5	0.7	0.6	0.6	0.5	0.4	0.4	0.7
c (Å)	96.2	95.8	95.8	96.2	96.3	95.7	96.5	93.4
Δc (Å)	−0.6	−1.0	−1.0	−0.6	−0.5	−1.1	−0.3	−3.4
Completeness of data (%)	71	92	72	72	69	84	80	84
R_{merge} (on I, %)	8.2	3.5	7.1	13.2	8.2	3.9	4.5	4.4
Isomorphous difference (%)	16.6	22.8	21.1	24.1	21.7	27.1	22.2	39.4
Refinement								
Reflections	10,953	15,363	11,915	11,083	11,942	11,361	17,451	12,441
Resolution (Å)	1.9	1.85	1.85	1.9	1.7	2.05	1.7	1.9
R-factor (%)	16.2	16.8	16.9	17.3	16.4	17.1	16.0	16.8
Δ_{bonds} (Å)	0.015	0.015	0.015	0.016	0.015	0.013	0.013	0.016
Δ_{angles} (°)	2.3	2.3	2.2	2.6	2.3	2.0	1.8	2.4
$\langle B \rangle$ (Å^2)	25	26	28	33	22	34	19	26

[a] The cell dimensions of wild-type lysozyme are $a = b = 61.2$ Å, $c = 96.8$ Å. Δa, Δb, and Δc are the changes in the cell dimensions of the mutant protein crystal relative to wild type. The average thermal factor $\langle B \rangle$ for the atoms within the backbone of the refined wild-type model is 19.7 Å^2. The isomorphous difference is the average difference between the observed structure amplitudes of the mutant and wild-type crystals.

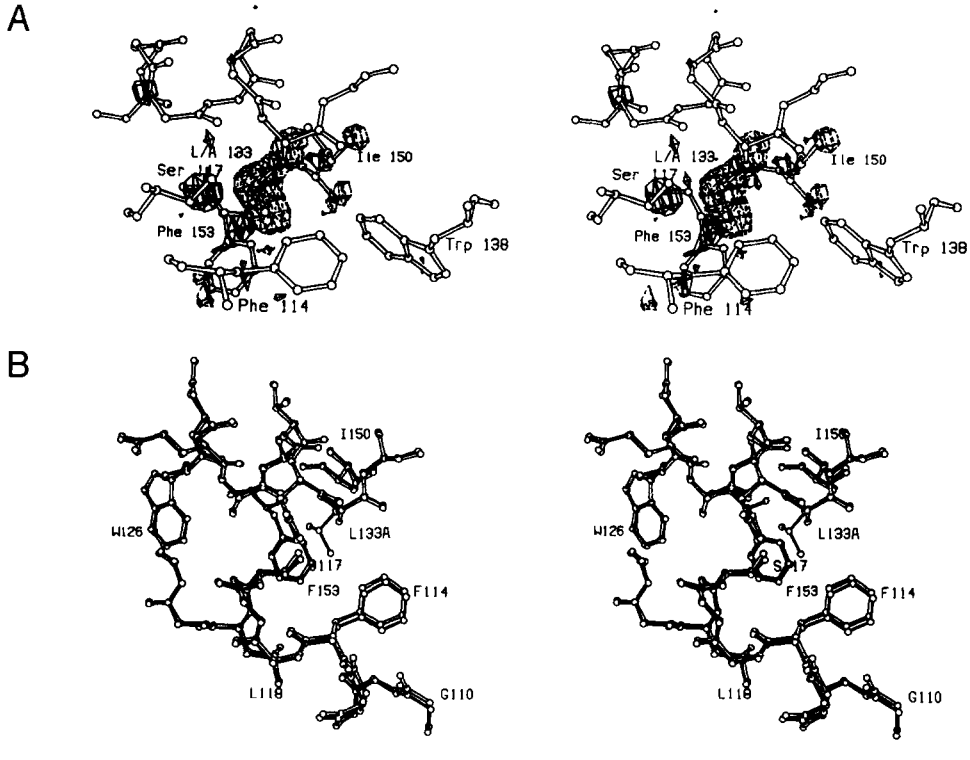

Fig. 2. **A**: Map showing the difference in density between L133A and wild-type lysozyme. Amplitudes ($F_{mut,obs} - F_{WT,obs}$) and phases calculated from the refined structure of wild-type lysozyme (Bell et al., 1991). Density contoured at 3.5σ, where σ is the rms density throughout the unit cell. Positive contours drawn solid; negative contours broken. Resolution as in Table 3. The coordinates of wild-type lysozyme are superimposed. **B**: Superposition of the refined structure of L133A (open bonds) on that of wild-type lysozyme (solid bonds). In all such comparisons the two sets of coordinates were superimposed so as to minimize the rms discrepancy between the main-chain atoms in the respective carboxy-terminal domains (i.e., residues 81–160).

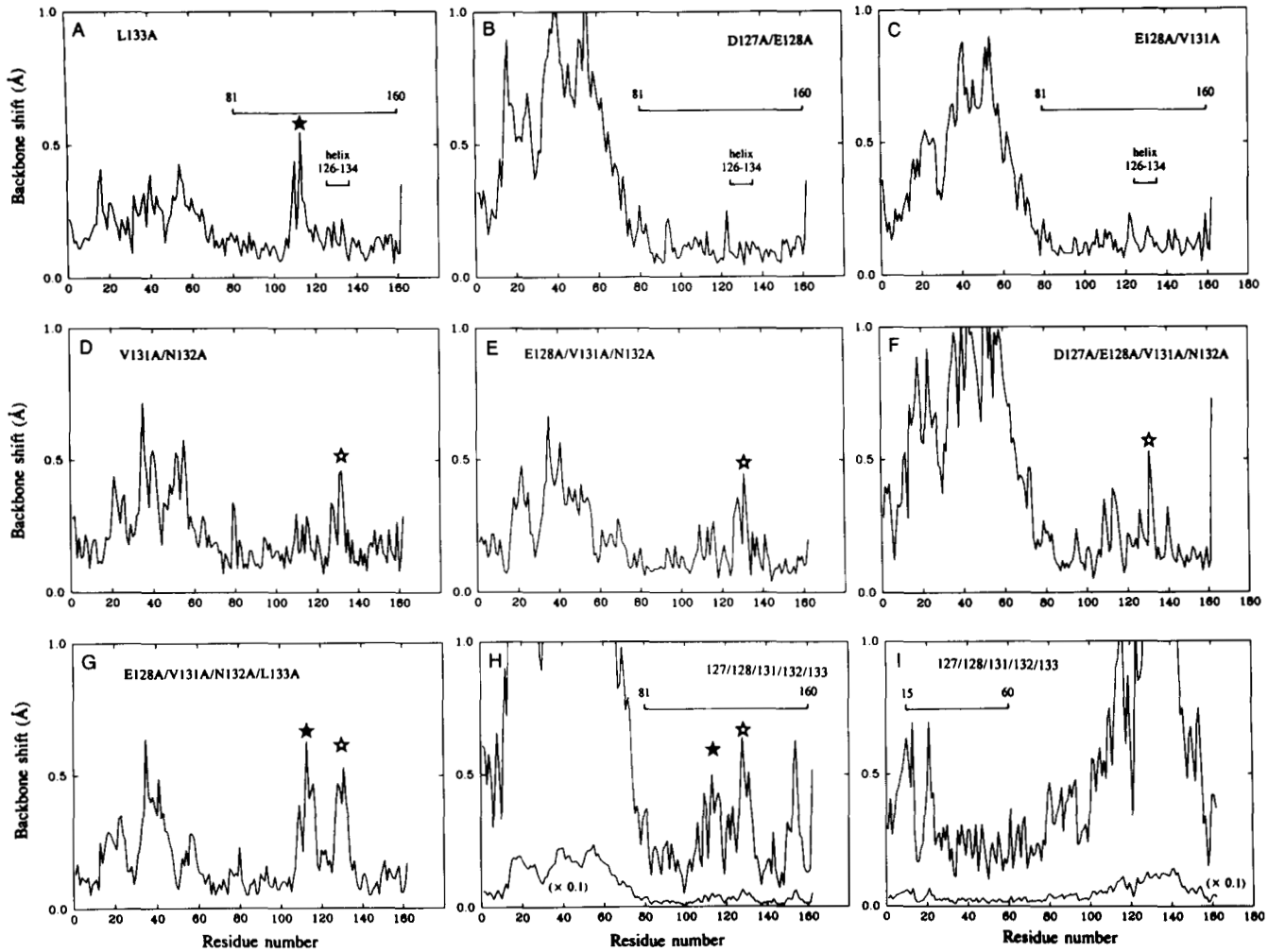

Fig. 3. Shift plots showing the displacement of the backbone atoms of each mutant relative to wild-type lysozyme. Each mutant structure was superimposed on the wild type so as to minimize the rms discrepancy between the respective backbone atoms in the carboxy-terminal domains (residues 81–160). For each amino acid the value plotted is the average (i.e., rms) discrepancy between the corresponding backbone atom (C^{α}, C^{β}, O, and N) in the mutant and wild-type structure. The single mutation Leu 133 → Ala causes backbone shifts in the vicinity of residues 109–114 and similar shifts are seen in all mutants that include this replacement (solid stars). Similarly, the mutation Asn 132 → Ala causes changes in the vicinity of residues 126–134 that are seen in all variants that include N132A (open stars). **A**: L133A; **B**: D127A/E128A; **C**: E128A/V131A; **D**: V131A/N132A; **E**: E128A/V131A/N132A; **F**: D127A/E128A/V131A/N132A; **G**: E128A/V131A/N132A/L133A; **H**: D127A/E128A/V131A/N132A/L133A; **I**: D127A/E128A/V131A/N132A/L133A; superposition based on the amino-terminal domains (residues 15–60). The large shift in Thr 21 is associated with a change in crystal contact between the backbone of Thr 21 and the side-chain of Trp 126 (see text).

of the α-helix and are relatively mobile. As expected, the structural changes associated with the replacement of each of these three residues with alanine are minimal.

In the respective difference maps (Figs. 5A, 6A) there is negative density, indicating the truncation of the three side chains to alanine. In the case of Glu 128, the side-chain carboxylate in the wild-type structure is very mobile, with thermal factors above 70 Å^2. This explains why the negative density in the difference maps does not extend to enclose the distal part of the side chain. Refinement confirms that the mutant structures are very similar to wild type (Figs. 5B, 6B). There is a slight rigid-body movement of the amino-terminal domain relative to the carboxy-terminal domain, which can be seen in the shift plots (Figs. 3, 4; Kinemage 3). Such movements have been seen in other mutant lysozymes and are usually accompanied by a change in the *c* cell edge, as is the case here ($\Delta c = -1.0$ Å). A similar, but smaller "hinge-bending" motion occurred for L133A (Fig. 3A), in which case the change in *c* was 0.6 Å. Based on superposition of atoms within their carboxy-terminal domains, the root-mean-square (rms) discrepancies between D127A/E128A and wild type and E128A/V131A and wild type are 0.11 Å and 0.12 Å, respectively.

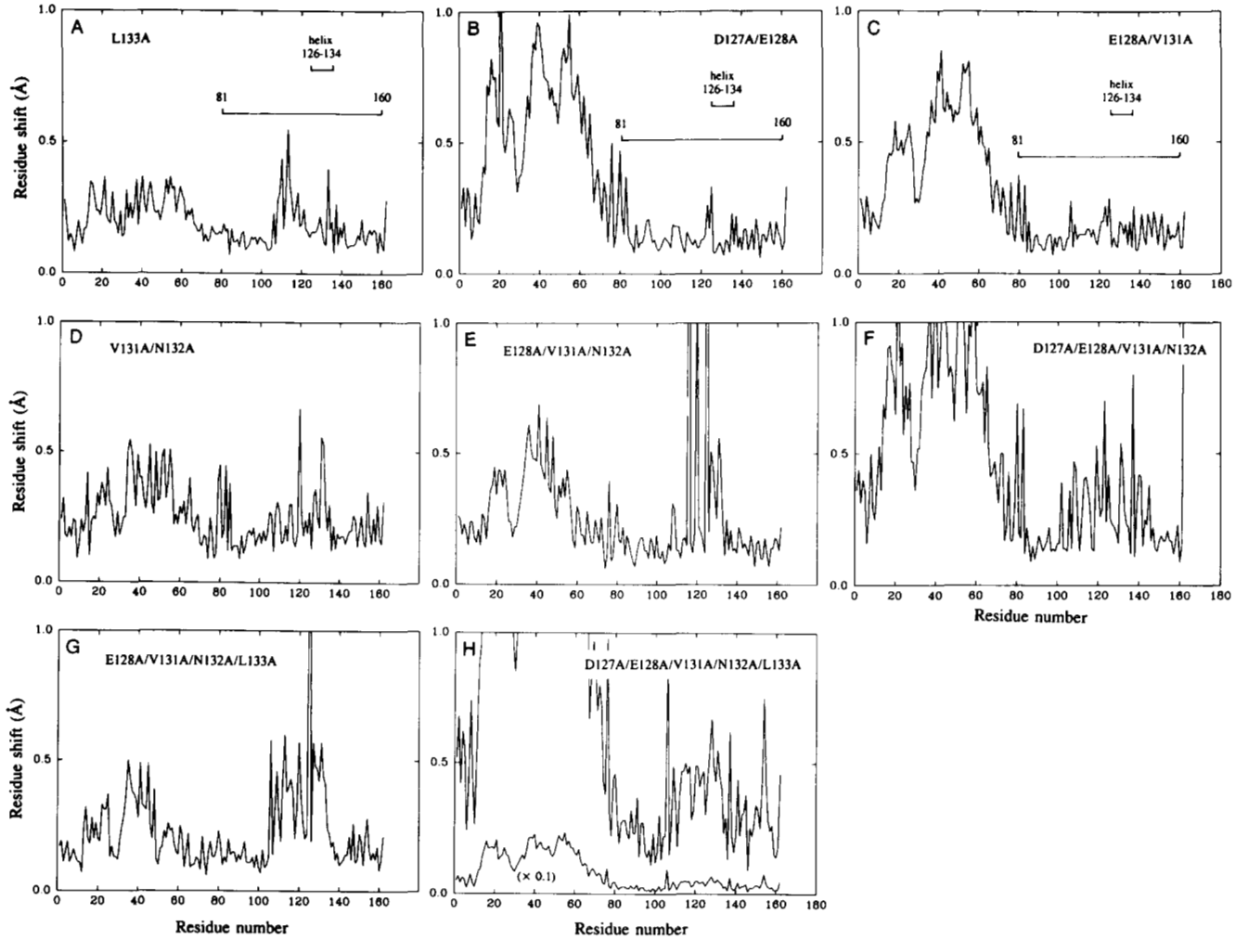

Fig. 4. Shift plots, as in Figure 3, showing the average displacement of the atoms in each residue of the mutant structure relative to wild type. **A**: L133A; **B**: D127A/E128A; **C**: E128/V131A; **D**: V131A/N132A; **E**: E128A/V131A/N132A; **F**: D127A/E128A/V131A/N132A; **G**: E128A/V131A/N132A/L133A; **H**: D127A/E128A/V131A/N132A/L133A.

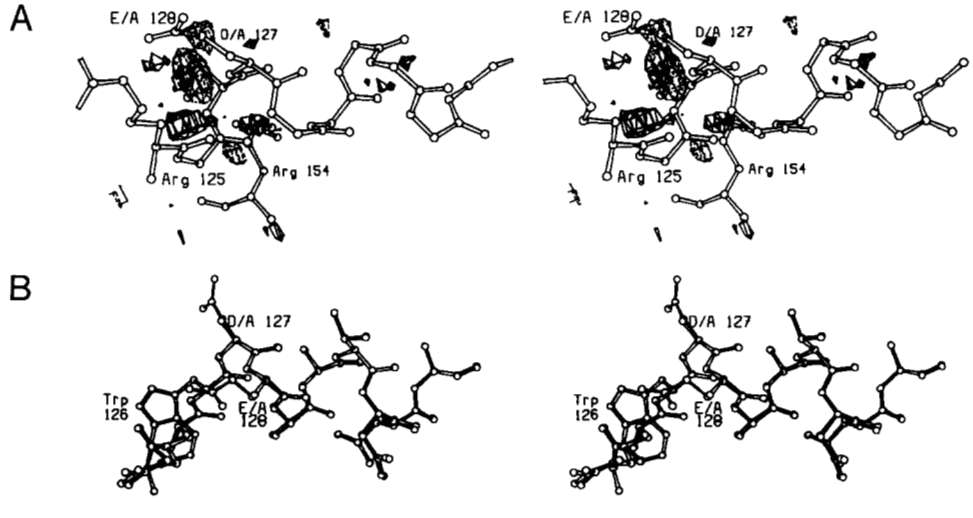

Fig. 5. **A**: Difference map, D127A/E128A minus wild-type lysozyme. All conventions as in Figure 2A. **B**: Superposition of D127A/E128A (open bonds) on wild type (solid bonds).

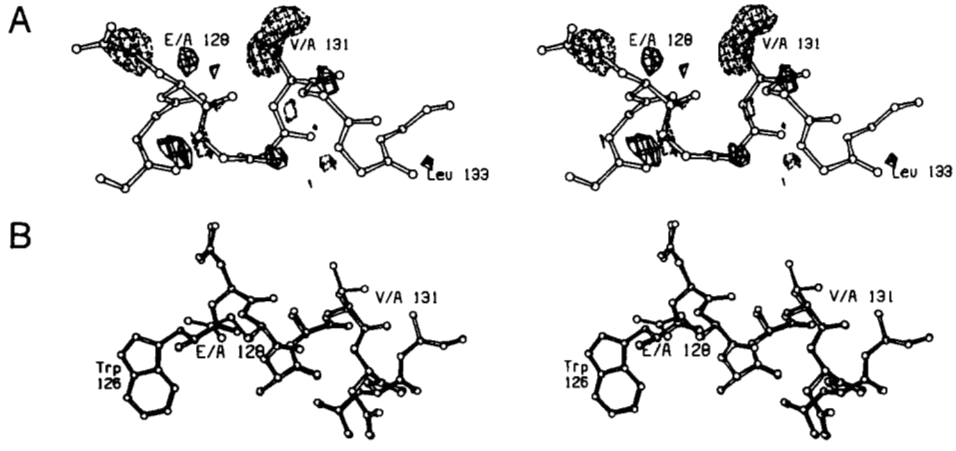

Fig. 6. **A**: Difference map, E128A/V131A minus wild-type lysozyme. All conventions as in Figure 2A. **B**: Superposition of D127A/E128A (open bonds) on wild type (solid bonds).

V131A/N132A and E128A/V131A/N132A

These two mutants will be considered together because they have two substitutions in common and were found to have extremely similar structures except for the truncation of Glu 128 in the latter case.

The difference maps for the two mutants (Figs. 7A, 8A) clearly show the expected negative density corre-

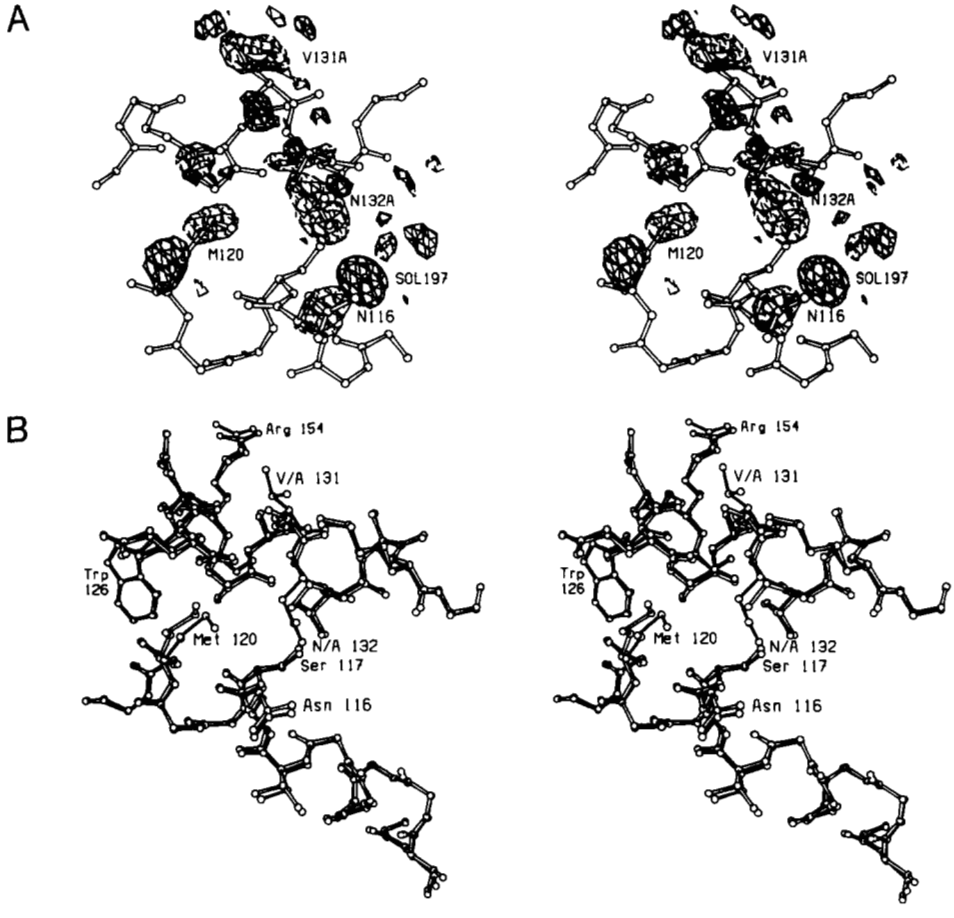

Fig. 7. **A**: Difference map, V131A/N132A minus wild-type lysozyme. All conventions as in Figure 2A. **B**: Superposition of V131A/N132A (open bonds) on wild type (solid bonds).

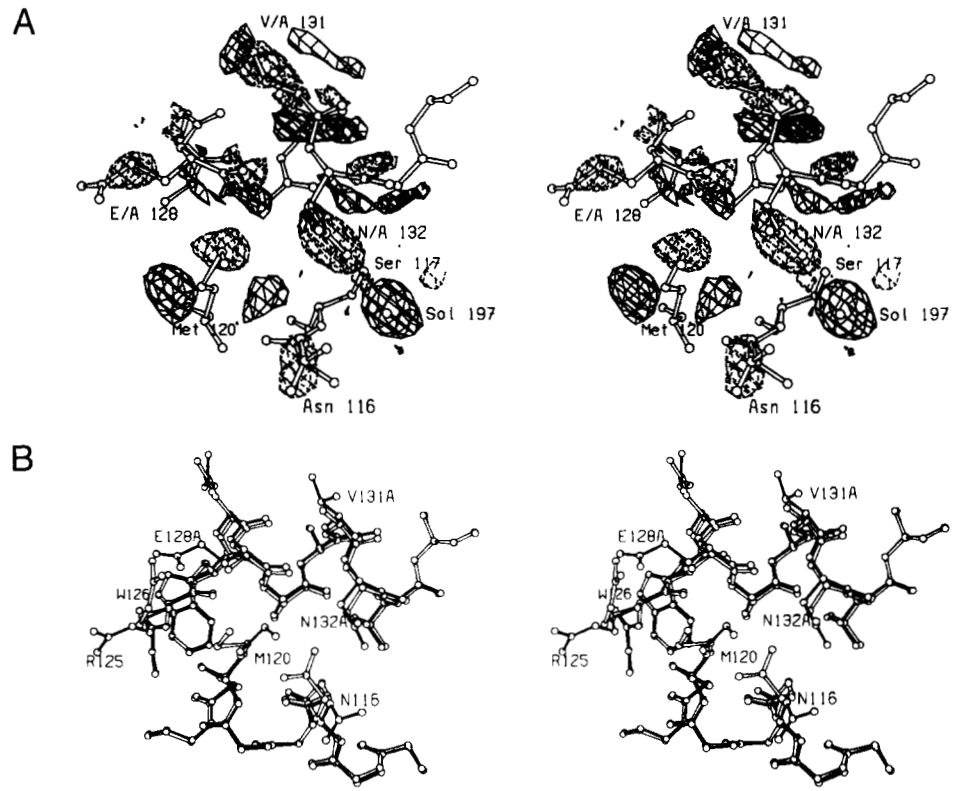

Fig. 8. **A**: Difference map, E128A/V131A/N132A minus wild-type lysozyme. All conventions as in Figure 2A. **B**: Superposition of E128A/V131A/N132A (open bonds) on wild type (solid bonds).

sponding to the substitutions of Val 131 and Asn 132 by alanine. As noted for D127A/E128A, the high mobility of Glu 128 causes the negative density at this site to be somewhat weaker. There is a strong positive density feature centered on the site occupied by solvent molecule #197 in the wild-type structure. This positive feature is a characteristic of all variants containing the Asn 132 → Ala substitution and is interpreted to be due to the replacement of solvent #197 by a chloride ion. It is presumed that the deletion of $O^{\gamma 1}$ of Asn 132 favors the binding of the anion. Positive and negative density features in the vicinity of the main-chain atoms of residues 126–134 indicate a shift of the α-helix as a whole (animated in Kinemage 4). For the triple mutant, especially (Fig. 8A), positive and negative features indicate substantial (>1 Å) rearrangements in the side-chain conformations of Asn 116 and Met 120. These are seen in the refined structure of the triple mutant (Fig. 8B) and in the shift plot (Fig. 4E). In the difference map for the double mutant (Fig. 7A), there are weaker density features suggesting that Asn 116 and Met 120 may tend to undergo the same conformational adjustment as seen in the triple mutant, but the refinement (Fig. 7B) indicates that, on average, Asn 116 and Met 120 retain an essentially wild-type configuration.

The superposition of the refined structures of V131A/N132A and E128A/V131A/N132A on wild type (Figs. 7B, 8B), as well as shift plots (Figs. 3D, 4E), shows the overall shift of the 126–134 α-helix by up to ~0.4 Å. Atoms within the 115–122 α-helix also move up to 0.25 Å. The larger movement, for helix 126–134, consists of a rotation of 3° about an axis that is approximately parallel to the axis of the 126–134 helix. The rotation is thought to be triggered by the substitution of Asn 132 by Ala, which removes a short hydrogen bond (2.5 Å) between $O^{\gamma 1}$ of the asparagine and O^{γ} of Ser 117, permitting repacking of the helix–helix interface (Zhang et al., 1991).

D127A/E128A/V131A/N132A

The difference map (Fig. 9A) and refined coordinates (Fig. 9B) show that the changes that occur in this mutant are similar to those seen in E128A/V131A/N132A. The α-helix undergoes a similar rotation of about 3°. A new solvent molecule occupies the site vacated by $N^{\gamma 2}$ of Asn 132. Also, the nearby solvent molecule (#197) present in wild-type lysozyme is replaced by a presumed chloride ion (Fig. 9A). The side chains of Asn 116 and Met 120 appear to retain an essentially wild-type conformation, although the thermal factors of these residues increase dramatically (29 to 70 $Å^2$ and 26 to 65 $Å^2$, respectively), indicating that the side chains are much less well ordered. It appears

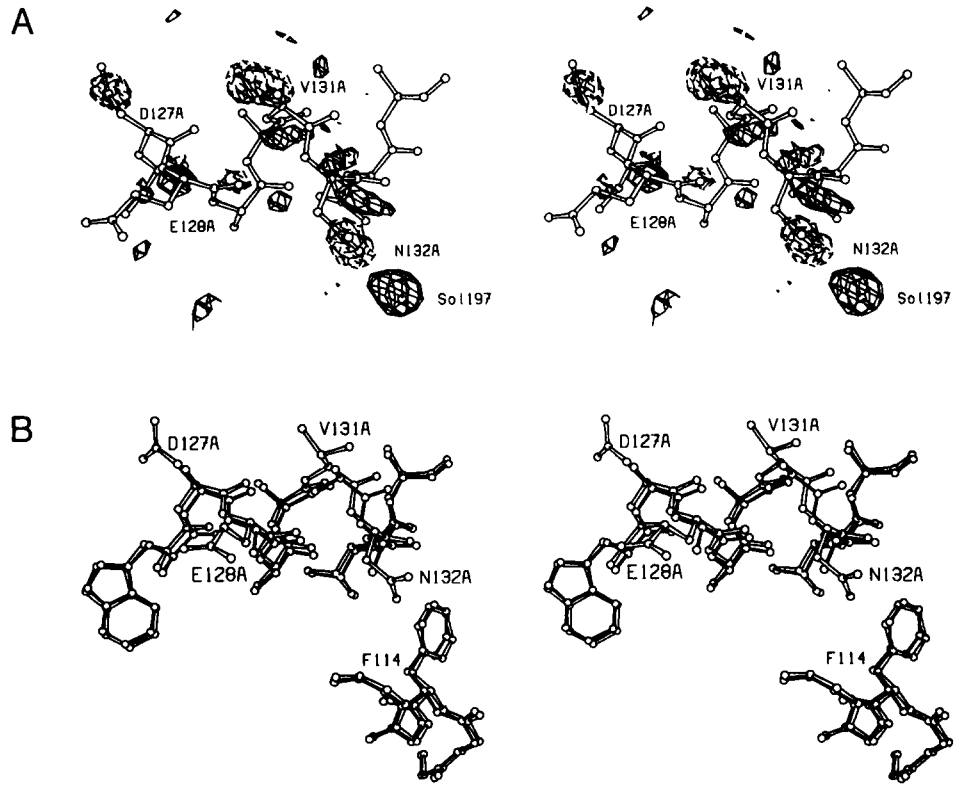

Fig. 9. **A**: Difference map, D127A/E128A/V131A/N132A minus wild-type lysozyme. All conventions as in Figure 2A. **B**: Superposition of D127A/E128A/V131A/N132A (open bonds) on wild type (solid bonds).

in this structure that both Cys 54 and Cys 97 form an adduct with β-mercaptoethanol (cf. Grütter et al., 1987; Bell et al., 1991). To accommodate this interaction with Cys 54, Arg 52 moves away and becomes more mobile.

E128A/V131A/N132A/L133A

The structural changes seen in this mutant are essentially a combination of those seen in E128A/V131A/N132A and L133A. The difference electron density map (Fig. 10A) has the expected negative density at the positions of the four truncated side chains. The other electron density features can be rationalized by the shift in the position of helix 126–134 (≤0.5 Å) and conformational changes in the side chains of Asn 116 and Met 120 and replacement of solvent #197 by a chloride ion. The shift plot (Fig. 3A) and the superimposed structures (Fig. 10B) also show the backbone shift (≤0.5 Å) in the vicinity of Phe 114. Also, Figure 4G shows a large apparent shift in the side chain of Arg 125. This residue is relatively mobile in both the wild-type and mutant structures.

D127A/E128A/V131A/N132A/L133A

One of the unusual characteristics of the crystals of this mutant is that the *c* cell dimension is 3.4 Å shorter than that of wild-type lysozyme (Table 2). This is the largest such change observed to date in over 140 mutant lysozymes that have been crystallized isomorphously with wild type. Independent precession photographs were used to confirm that the short cell edge occurred in other crystals of this mutant and was not, for example, due to partial dehydration of the crystal used for data collection. Because of the 3% change in cell dimension, the average difference between the structure amplitudes of the mutant and wild-type lysozyme was unusually high (39%) (Table 3). For the same reason the initial difference density map (Fig. 11A) was also very noisy. Nevertheless, negative density can be seen at the locations of those residues replaced by alanine. As in all cases, refinement of the mutant structure commenced with several cycles of rigid-body refinement (Dao-pin et al., 1991). In the present instance such a procedure was practically essential.

The superposition of the mutant structure of wild type (Figs. 11B, 3H, 4H) shows that it has coordinate shifts of 0.5 Å or so through much of the carboxy-terminal domain. Most of these rearrangements were seen in the constituent mutants but, in addition, there is a structural change of about 0.6 Å at Arg 154. This change was not seen in D127/E128A or in 128/131/132/133 and seems to be a case where the combined mutant provides additional freedom for Arg 154 to move that it does not enjoy in the

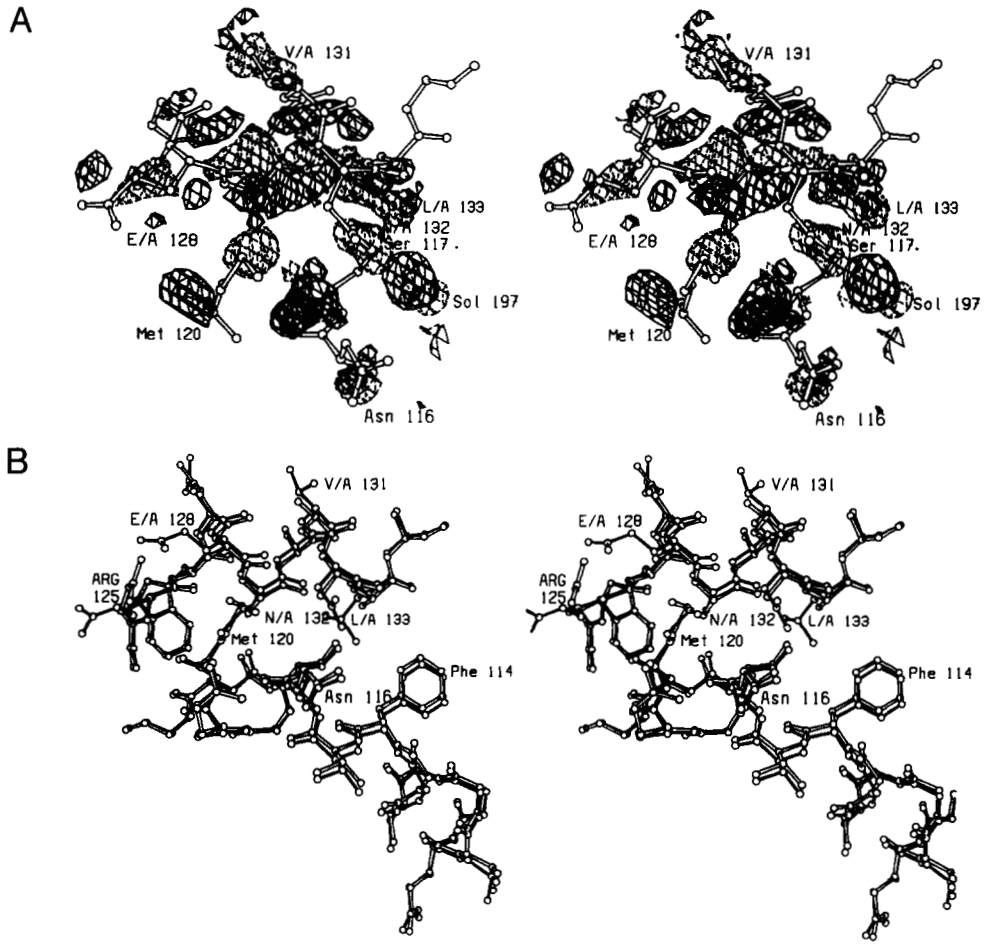

Fig. 10. **A**: Difference map, E128A/V131A/N132A/L133A minus wild-type lysozyme. All conventions as in Figure 2A. **B**: Superposition E128A/V131A/N132A/L133A (open bonds) on wild type (solid bonds). The difference map (Fig. 10A) suggests that both Met 120 and Asn 116 change their conformations in the mutant structure. The refinement indicates that these residues each are distributed between two different conformations; that shown in the figure corresponds to the conformation closest to wild-type lysozyme.

constituent mutants. It provides an example of structural changes in a mutant that are not a simple combination of those of its constituent mutations. In other words, there is an interaction between the constituent substitutions.

In the 127/128/131/132/133 mutant the accuracy of the structure in the vicinity of the cavity created by the replacement of Leu 133 with Ala is somewhat uncertain. In the final $(2F_o - F_c)$ electron density map the definition of the aromatic ring of Phe 153 is not perfect. Also, 2.5 Å away from the refined position of the benzyl group, in the space vacated by the Leu 133 side chain, there is an electron density feature that is of height 5σ in the corresponding $(F_o - F_c)$ difference map. It seems unlikely that this density corresponds to an alternative (t) conformation of Phe 153 because of steric constraints. The possibility exists, therefore, that the electron density feature might indicate a water molecule in this essentially hydrophobic cavity, but we do not regard this as likely as there is no polar atom within 4 Å. A much more reliable indication is provided by the mutant structure with the single replacement Leu 133 → Ala. In this case the structure in the region of the substitution is well defined and there is no evidence whatsoever to suggest that the created cavity contains a bound solvent molecule.

Discussion

Tolerance of a polyalanine helix

The major finding of the present work is that a series of eight consecutive alanines within the amino acid sequence of T4 lysozyme does not interfere with folding or function. This supports the notion that the folding of a protein may be determined by the interactions between a subset of key amino acids (e.g., those that form the core) and that the remainder (which may constitute a relatively large fraction of the amino acid sequence) are relatively unimportant. Other evidence in support of this idea in-

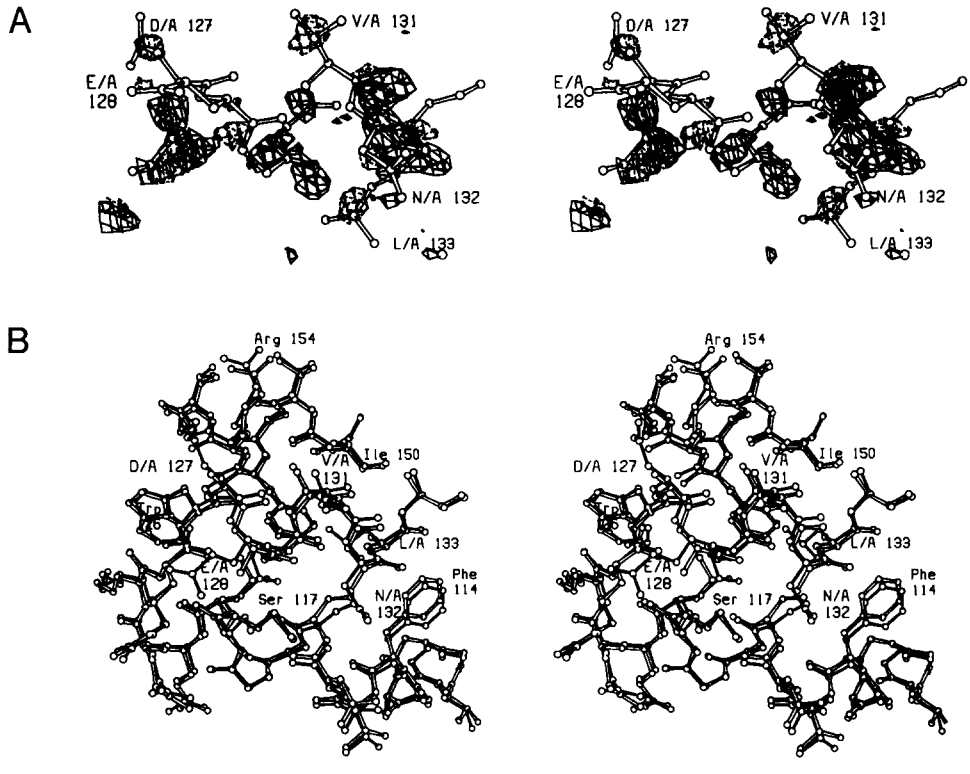

Fig. 11. **A**: Difference map, D127A/E128A/V131A/N132A/L133A minus wild-type lysozyme. All conventions as in Figure 2A. **B**: Superposition of D127A/E128A/V131A/N132A/L133A (open bonds) on wild type (solid bonds).

cludes the demonstration by Sauer and coworkers that amino acids in a given protein can have a low "information content" (Bowie et al., 1990). Also, amino acid substitutions of mobile solvent-exposed residues on the surface of a protein generally have little effect on stability (Hecht et al., 1986; Alber et al., 1987). In experiments parallel to those reported here, Heinz et al. (1992) have constructed a mutant lysozyme with 10 consecutive alanines (residues 40–49) in a different α-helix and have shown that that variant also folds normally.

Independence of substitutions: Energetics

It was previously shown that substitution of alanine at the three relatively solvent-exposed sites, Glu 128, Val 131, and Asn 132, increased the thermostability of T4 lysozyme (Zhang et al., 1991). The increase in stability at the three sites was found to be approximately additive, although there was a slight synergistic effect that was interpreted to be due to an interaction between the E128A and N132A substitutions. Table 4 gives an overall summary in which an energy term is ascribed to each single alanine substitution. These energies were either measured directly or inferred by difference, as described by Zhang et al. (1991). By summing the individual energy terms and including the interaction term for those variants that include both E128A and N132A, one can predict the change in stability expected for each of the multiple replacements. For E128A/V131A, 128/131/132, and 127/128/131/132, the agreement between the observed energy and the sum of the constituents is good. For the mutations that include L133A, the agreement is poorer, but it should be noted that L133A is a relatively unstable protein, and in such cases it is more difficult to obtain accurate values for $\Delta\Delta G$ (Table 2). In general terms, the results support the principle of additivity and suggest that each of the substitutions acts essentially independently. Such independence would not necessarily be expected for substitutions involving pairs of amino acids that are coupled via interactions through the rest of the protein. Suppose, for example, that two amino acids in the same α-helix each made contact with the core of the protein. A substitution of one amino acid might alter the alignment of the α-helix relative to the rest of the protein, which, in turn, would affect the consequences of a substitution of the second amino acid. In such a case substitutions at the two sites would be coupled even though there need not be direct contact between the amino acids in question. This situation occurs with the replacements E128A and N132A, although in this case the estimated interaction energy is relatively weak (~0.2 kcal/mol) (Zhang et al., 1991) (Table 4). Because of the uncertainty in the estimation of $\Delta\Delta G$ for the destabilizing single replacement Leu 133 → Ala (Table 4), we cannot exclude

Table 4. *Additivity of energies of stabilization*[a]

Mutant	Stabilization observed experimentally $\Delta\Delta G$ (kcal/mol)	Stabilization inferred from constituent mutations $\Delta\Delta G$ (kcal/mol)
(D127A)		0.08
E128A	0.16	
V131A	0.27	
(N132A)		0.30
L133A	−4.19	
D127A/E128A	0.24	
E128A/V131A	0.44	0.43
V131A/N132A	0.57	
128/131/132	0.91	0.73 (0.91)
127/128/131/132	1.01	0.81 (0.99)
128/131/132/133	−2.59	−3.46 (−3.28)
127/128/131/132/133	−2.27	−3.38 (−3.20)

[a] The energies of stabilization of the multiple mutants are compared with the sums of energies of stabilization of the constituent replacements. The left-hand column gives the experimentally observed energies of stabilization for each of the mutant proteins ($\Delta\Delta G$ from Table 2). Mutations D127A and N132A were not constructed as single replacements so that in these two cases the energy values are inferred by difference from the values for D127A/E128A and E128A and V131A/N132A and V131A. The sum of the energies for E128A, V131A, and N132A is 0.73 kcal/mol (as shown above), but better agreement with the experimental value is obtained by assuming that there is an interaction energy of 0.18 kcal/mol between E128A and N132A due to a structural rearrangement (see Zhang et al., 1991). This results in an energy sum of 0.91 kcal/mol, shown above in parentheses. Similarly, multiple mutants 128/131/132/133 and 127/128/131/132/133 also include both E128A and N132A, so the inferred stabilization energy is shown as the simple sum of the constituents (without parentheses) and with the 0.18-kcal/mol interaction energy term included (in parentheses).

the possibility that there is some cooperativity in the multiple mutants that include this substitution.

Table 4 suggests that the four alanine substitutions—D127A, E128A, V131A, and N132A—increase protein stability (at pH 2.0) and that the replacement of the buried Leu 133 is substantially destabilizing.

Independence of substitutions: Structure

An overall impression of the conformational changes associated with the different mutants is given by the shift plots shown in Figures 3 and 4 and also the comparisons of the coordinates with wild-type lysozyme (Table 5). Because the different mutations are associated with changes in the "hinge-bending angle" between the amino-terminal and carboxy-terminal domains the superposition of each structure on wild type was based on the main-chain atoms of the carboxyl domain (i.e., residues 81–160). This is the domain in which the polyalanine helix is located. Similar superpositions were also carried out for each pair of mutant structures, yielding the discrepancies shown in Table 6. Not surprisingly, mutants D127A/E128A and E128A/V131A, which involve fully solvent-exposed residues, have structures most similar to the wild type (rms discrepancy, Δ, of 0.11–0.12 Å) and to each other (Δ = 0.13 Å). These three structures can be considered identical, within experimental error, except in the immediate vicinity of the substitution sites (Fig. 3B,C). As discussed under Results, the replacement Asn 132 → Ala is associated with a shift of the 126–134 helix. This can be seen in all the variants that include N132A (Fig. 3D–H). Similarly, the replacement Leu 133 → Ala is associated with a shift in the α-helical residues 109–114. This shift is clearly seen in all the variants that include L133A (Fig. 3A,G,H). This indicates quite clearly that the major structural changes associated with the different mutations are independent. The observation that the structural changes seen in the multiple mutants are the sum of those seen in the individual mutants is consistent with the additivity also seen in the free energies of stabilization (Table 4).

Large-scale changes in conformation

Superposition of the amino-terminal domain of each mutant on wild type shows that this part of the lysozyme structure is, in general, very similar in each structure (data not shown except for Fig. 3I, see below). This confirms that the overall difference between each mutant and wild type consists essentially of two parts. First there are adjustments within the carboxy-terminal domain that can include relatively extended main-chain shifts up to 0.5–0.6 Å (e.g., Fig. 3H). Second there is the rigid-body movement of the amino-terminal domain relative to the carboxyl-terminal domain, which, in the case of 127/128/131/132/133, corresponds to a rotation of 3.6° (Fig. 12). In this case, however, as can be seen in Figure 3I, there are some parts of the amino-terminal domain that do readjust in the mutant structure. These include residues 7–13 and 18–23. The latter is a hairpin or loop structure, which, in wild-type lysozyme, has relatively high thermal factors, indicating higher than average mobility. In the wild-type crystal lattice, there is an intermolecular hydrogen bond (3.1 Å) between the carbonyl oxygen of Thr 21 and the indole nitrogen of Trp 126 (Fig. 13; Kinemage 5). In the mutant structure this hydrogen bond is broken, and the interatomic distance increases to 4.3 Å. Instead, a new intermolecular hydrogen bond (3.1 Å) is formed between the indole nitrogen and the carbonyl oxygen of Asp 20 (Fig. 13). Associated with this change, the side chain of Thr 21 rotates from the g^- conformation in wild type to g^+ in the mutant. Thus, the 3.4-Å decrease in the *c* cell edge is associated with hinge-bending of the two domains within the lysozyme molecule, a distinct change in a crystal-packing contact, and, as well, localized adjustments of the protein structure in the vicinity of the contact.

Although there is no direct evidence, we do not believe that the change in hinge-bending angle is an intrinsic property of the mutant lysozyme. Rather, we suggest that

Table 5. *Root-mean-square differences between the coordinates of polyalanine mutants and wild-type lysozyme*

Mutant	Discrepancy for residues compared (Å)			
	1–162 (all atoms)	1–162 (main chain)	81–160 (all atoms)	81–160 (main chain)
133	0.18	0.16	0.18	0.16
127/128	0.26	0.22	0.16	0.11
128/131	0.22	0.19	0.17	0.12
131/132	0.25	0.21	0.24	0.18
128/131/132	0.37	0.18	0.46	0.16
127/128/131/132	0.39[a]	0.28	0.29	0.19
128/131/132/133	0.29	0.20	0.35	0.22
127/128/131/132/133	0.53	0.47	0.36	0.28

[a] The side chain of Arg 52, which moves in association with modification of Cys 54, is not included in the comparison (see text).

Table 6. *Root-mean-square difference between the backbone coordinates (in Å) for residues 81–160 in each of the mutant structures*

	Wild type	133	127/128	128/131	131/132	128/131/132	127/128/ 131/132	128/131/ 132/133	127/128/ 131/132/133
Wild type		0.16	0.11	0.12	0.18	0.16	0.19	0.22	0.28
133			0.17	0.18	0.20	0.18	0.19	0.18	0.25
127/128				0.13	0.19	0.16	0.19	0.23	0.28
128/131					0.16	0.16	0.19	0.24	0.29
131/132						0.14	0.18	0.19	0.25
128/131/132							0.15	0.15	0.24
127/128/131/132								0.18	0.23
128/131/132/133									0.19
127/128/131/132/133									

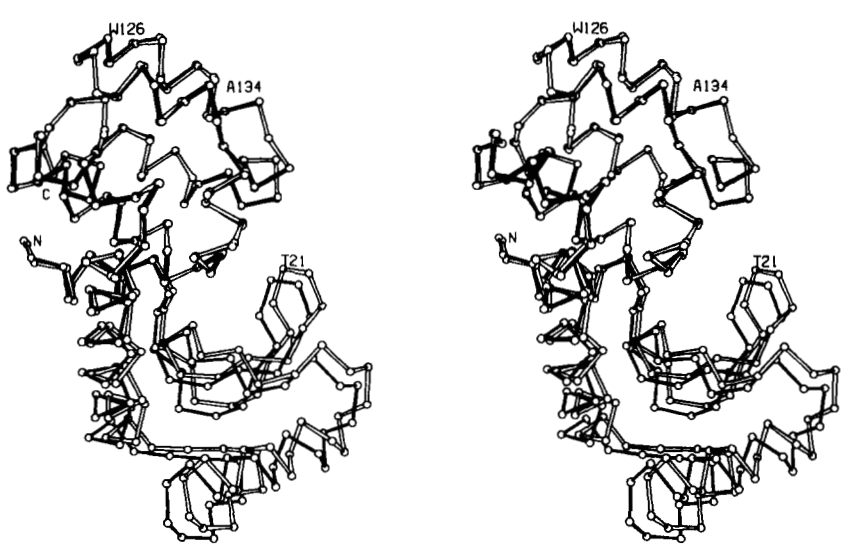

Fig. 12. Stereo drawing showing the "hinge-bending" motion of mutant D127A/E128A/V131A/N132A/L133A (open bonds) relative to wild type (solid bonds). The superposition of the two structures is to optimize the agreement between their carboxy-terminal domains. The polyalanine helix includes residues 127–134. Trp 126 of one molecule and Thr 21 of another molecule participate in the contact within the crystal lattice (see text and Fig. 13).

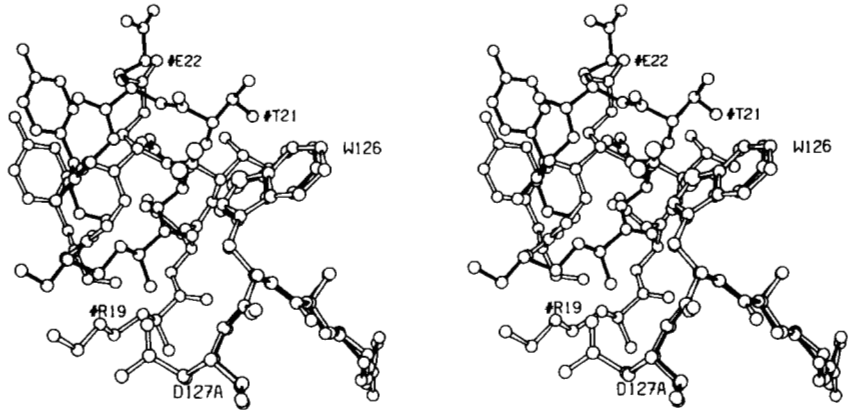

Fig. 13. Stereo drawing showing the change in crystal contact associated with the penta-alanine substitution. In wild-type lysozyme (solid bonds) there is a hydrogen bond between the indole nitrogen of Trp 126 (W126) and the carbonyl oxygen of Thr 21 in a neighboring molecule (differentiated by the # symbol) in the crystal lattice. In the D127A/E128A/V131A/N132A/L133A mutant structure (open bonds) the intermolecular hydrogen bond occurs between the indole nitrogen and the carbonyl oxygen of Asp 20. In this figure the coordinates were taken from the respective crystal structures and aligned so as to optimize the superposition of the backbone atoms of residues 125–127.

the structural changes in the vicinity of the polyalanine helix favor an alternative crystal contact, and the hinge-bending angle adjusts to facilitate this new contact. Substantial variability in hinge-bending has been observed in two other T4 lysozyme variants, Met 6 → Ile (Faber & Matthews, 1990) and Ile 3 → Pro (unpubl. results). It is presumed in the case of these variants that it requires very little energy to change the hinge-bending angle (Faber & Matthews, 1990), and the present results tend to suggest that this is true in general, as the mutations described here are well away from the hinge-bending region (Fig. 1).

Structure of the polyalanine helix

The polyalanine helix in the mutant 127/128/131/132/133 and in the other variants is very similar to that of wild type except for the truncation of the mutated residues. One question is whether the geometry of the α-helix becomes more regular as its sequence becomes more homogeneous. In the most extreme case two full turns of the α-helix consist exclusively of alanine residues. Helix geometry was investigated in several ways, first by determining the spread in the (ϕ,ψ) values (Table 7). To some degree the replacement of the buried residue Leu 133 seems to make the helix less regular (i.e., increases $\sigma(\phi)$ and $\sigma(\psi)$), and the subsequent replacements tend to restore regularity, but this trend is not especially compelling. In terms of the variations of the hydrogen bond lengths within the α-helix (Table 8) it also appears that the Leu 133 → Ala substitution disrupts the helix somewhat, and the subsequent substitution of additional alanines makes it more regular, in fact substantially more so than the helix in the wild-type structure. Finally, an attempt was made to compare the polyalanine helix with an ideal α-helix. One of the difficulties in such a comparison is to define an ideal helix. Table 9 summarizes two different types of comparisons. In the first test, the backbone atoms (C^{α}, C, N, O) of residues 127–133 in the different mutant structures were compared with a model polyalanine α-helix in which every residue has ($\phi = -57°$, $\psi = -47°$) (Arnott & Wonacott, 1966). In the second test, the α-helix was compared with itself, but translated by a single residue (i.e., residues 127–132 were superimposed on and compared with residues 128–133). The idea of the latter comparison was that it would help allow for a situation in which the overall helix was slightly bent. In particular, it is known (Blundell et al., 1983) that buried hydrogen bonds tend to be shorter than those exposed to solvent, and this is true for α-helix 126–134 of T4 lysozyme (Table 8). The comparisons shown in Table 9 tend to support the general trend discussed above, namely that the Leu 133 → Ala replacement makes the helix less regular, and that multiple alanine replacements restore regularity. A polyalanine helix in solution might be expected to have a completely regular conformation. Here, however, not all alanines are equivalent. Some are solvent-

Table 7. *Variation of (ϕ,ψ) within the polyalanine helix*[a]

Residue	ϕ (°)	ψ (°)		
A. Ramachandran angles in wild-type lysozyme, residues 126–134				
Trp 126	−52.7	−54.8		
Asp 127	−62.6	−42.7		
Glu 128	−66.2	−39.4		
Ala 129	−64.9	−38.8		
Ala 130	−59.2	−45.0		
Val 131	−64.3	−43.5		
Asn 132	−67.4	−37.5		
Leu 133	−64.4	−29.6		
Ala 134	−72.8	−16.1		
Protein	$\langle\phi\rangle$ (°)	$\langle\psi\rangle$ (°)	$\sigma(\phi)$ (°)	$\sigma(\psi)$ (°)
B. Average (ϕ,ψ) values in mutant lysozymes, residues 127–133				
Wild type	−64.1	−39.5	2.5	4.8
L133A	−65.6	−37.3	4.7	8.4
D127A/E128A	−64.1	−39.8	4.8	4.6
E128A/V131A	−65.3	−38.9	6.4	3.7
V131A/N132A	−64.6	−40.3	7.7	2.8
E128A/V131A/N132A	−64.3	−39.3	4.9	3.4
127/128/131/132	−62.1	−40.8	5.8	4.9
128/131/132/133	−67.7	−37.0	4.1	4.1
127/128/131/132/133	−65.6	−39.2	3.5	4.8

[a] $\langle\phi\rangle$ and $\langle\psi\rangle$ are the rms values of ϕ and ψ, and $\sigma(\phi)$ and $\sigma(\psi)$ are the variations for the residues within the α-helix. In calculating the average values of ϕ and ψ the capping residues were deleted.

Table 8. *Helical hydrogen bond lengths within polyalanine helices*

Atom pair		Bond length (Å)
A. Hydrogen bond lengths within α-helix 126–134 in wild-type lysozyme		
O Trp 126	N Ala 130	3.09
O Asp 127	N Val 131	3.21
O Glu 128	N Asn 132	3.08
O Ala 129	N Leu 133	2.78
O Ala 130	N Ala 134	3.38

Protein	⟨*d*⟩ (Å)	σ(*d*) (Å)
B. Variation in hydrogen bond length in mutant structures		
Wild type	3.11	0.20
L133A	3.12	0.23
D127A/E128A	3.16	0.17
E128A/V131A	3.11	0.20
V131A/N132A	3.18	0.17
E128A/V131A/N132A	3.05	0.14
127/128/131/132	3.16	0.16
128/131/132/133	3.08	0.11
127/128/131/132/133	3.04	0.13

Table 9. *Comparison of polyalanine helix with an ideal helix and with a "translated" helix*

Protein	Agreement between residues 127–133 and an ideal helix ($\phi = -57°$, $\psi = -47°$)[a] (Å)	Agreement between residues 127–132 and residues 128–133 (Å)
Wild type	0.248	0.233
L133A	0.262	0.279
D127A/E128A	0.261	0.233
E128A/V131A	0.226	0.212
V131A/N132A	0.257	0.270
E128A/V131A/N132A	0.194	0.164
127/128/131/132	0.220	0.208
128/131/132/133	0.221	0.127
127/128/131/132/133	0.234	0.175

[a] If the calculation is repeated with an "average" α-helix ($\phi = -62°$, $\psi = -41°$) (Barlow & Thornton, 1988), the individual discrepancies increase by about 0.04 Å, but the overall trend is the same.

exposed and some are buried. The observed conformation presumably reflects a compromise between the tendency of the repeated alanine sequence to make the helix more regular and the constraints imposed by the contacts of the α-helix with the rest of the protein.

Surface and solvent structure

As noted above, the substitution of up to five alanines has no apparent effect on the purification of the protein or on its aggregation properties (as inferred from its behavior during purification and crystallization). Table 10

Table 10. *Area of residues 126–134 accessible to solvent*[a]

Mutant	Surface area for atoms specified (Å²)			
	Carbon	Oxygen	Nitrogen	Total
Wild type	218	172	45	434
133	219	174	46	439
127/128	268	23	49	341
128/131	195	102	46	344
131/132	176	167	22	366
128/131/132	183	96	22	301
127/128/131/132	236	20	27	283
128/131/132/133	196	98	26	320
127/128/131/132/133	256	19	29	304

[a] Areas accessible to solvent were calculated using the method of Lee and Richards (1971) with a probe radius of $r = 1.4$ Å.

shows the total accessible surface area of residues 126–134, given by atom type. The most significant change is in the reduction in the accessible surface area attributed to oxygen atoms due, in particular, to the loss of Asp 127 and Glu 128. Although up to five alanines are substituted, the hydrocarbon surface area exposed to solvent remains roughly constant.

Of the five mutation sites, the first three, Asp 127, Glu 128, and Val 131, are fully solvent exposed. Asn 132 is partly inaccessible to solvent, whereas Leu 133 is fully buried. For the full-exposed residues, replacement with alanine would not be expected to result in the binding of additional solvent molecules, and none is observed. Similarly, there is no evidence of solvent bound within the hydrophobic cavity created by the single Leu 133 → Ala replacement (but see the comment under Results regarding mutant 127/128/131/132/133).

The only mutants for which there is clear evidence for binding of an additional solvent molecule are those that include the replacement of Asn 132 → Ala. In E128A/V131A/N132A, 127/128/131/132, and 128/131/132/133 there is a water molecule that occupies approximately the same position as $N^{\gamma 2}$ of Asn 132. In the wild-type crystal structure $N^{\gamma 2}$ of Asn 132 makes a hydrogen bond (3.0 Å) to $O^{\epsilon 2}$ of Glu 45 in a neighboring molecule. The bound solvent molecule in the mutant structures makes a similar hydrogen bond to Glu 45.

Helix 126–134 is amphiphilic. In the wild-type structure there are four water molecules that respectively hydrogen bond to the carbonyl oxygens of Asp 127, Glu 128, Ala 130, and Val 131. These hydrogen bonds have an average length of 2.9 ± 0.1 Å. The average of the angles formed by the carbonyl carbon, carbonyl oxygen, and the water molecule is 116 ± 7°. For Asp 127, Glu 128, and Val 131 the average of the pseudo torsion angles formed by the α-carbon, carbonyl carbon, carbonyl oxygen, and water molecule is 22 ± 3°. All of these values are very close to those normally observed for water molecules bound to

the solvent-exposed residues in the center of an amphiphilic α-helix (Blundell et al., 1983; Baker & Hubbard, 1984; Barlow & Thornton, 1988). Because Ala 130 is partially buried it prevents the bound solvent (#216) at this position from having the standard 22° angle. Instead, the pseudo torsion angle is 107°. None of the above binding patterns of solvent is altered in any of the mutant structures (except that the thermal factors of the solvent molecules vary somewhat). In addition all of the water molecules within 3.5 Å of the side chains of residues 127, 128, 131, 132, and 133 of wild-type lysozyme retain reasonable B-values (below 65 $Å^2$) in the mutant structures.

The overall result, therefore, is that the presence of the alanine substitutions does not alter the solvent structure on the surface of the protein except for the one case where a solvent molecule replaced a hydrogen-bonding function on a substituted amino acid.

Methods

Methods for generation and purification of the mutant lysozymes, as well as thermodynamic and crystallographic analysis, were as described previously (Dao-pin et al., 1990; Zhang et al., 1991). The polyalanine variants were obtained by standard procedures, although in DNA sequencing it was necessary to use 7-deaza-dGTP instead of dGTP to prevent the GC-rich region (. . . GCX GCX GCX . . .) from forming secondary structure.

Acknowledgments

We thank Joan Wozniak and Sheila Pepiot for protein preparations, Joel Lindstrom for CD measurements, Dr. Larry Weaver for his help with the data collection, and Dr. Robert DuBose for advice on sequencing. This work was supported in part by grants from the NIH (GM21967) and the Lucille P. Markey Charitable Trust.

References

Alber, T., Dao-pin, S., Nye, J.A., Muchmore, D.C., & Matthews, B.W. (1987). Temperature-sensitive mutations of bacteriophage T4 lysozyme occur at sites with low mobility and low solvent accessibility in the folded protein. *Biochemistry 26*, 3754–3758.

Arnott, S. & Wonacott, A.J. (1966). Atomic coordinates for an α-helix: Refinement of the crystal structure of α-poly-L-alanine. *J. Mol. Biol. 21*, 371–383.

Baker, E.N. & Hubbard, R.E. (1984). Hydrogen bonding in globular proteins. *Prog. Biophys. Mol. Biol. 44*, 97–179.

Barlow, D.J. & Thornton, J.M. (1988). Helix geometry in proteins. *J. Mol. Biol. 201*, 601–619.

Becktel, W.J. & Schellman, J.A. (1987). Protein stability curves. *Biopolymers 26*, 1859–1877.

Bell, J.A., Wilson, K.P., Zhang, X.-J., Faber, H.R., Nicholson, H., & Matthews, B.W. (1991). Comparison of the crystal structure of bacteriophage T4 lysozyme at low, medium and high ionic strengths. *Proteins Struct. Funct. Genet. 10*, 10–21.

Blundell, T., Barlow, D., Borkakoti, N., & Thornton, J. (1983). Solvent-induced distortions and the curvature of α-helices. *Nature 306*, 281–283.

Bowie, J.U., Reidhaar-Olson, J.F., Lim, W.A., & Sauer, R.T. (1990). Deciphering the message in protein sequences: Tolerance to amino acid substitutions. *Science 247*, 1306–1310.

Brandts, J.F. & Hunt, L. (1967). The thermodynamics of protein denaturation. III. The denaturation of ribonuclease in water and in aqueous urea and aqueous ethanol mixtures. *J. Am. Chem. Soc. 89*, 4826–4838.

Dao-pin, S., Alber, T., Baase, W.A., Wozniak, J.A., & Matthews, B.W. (1991). Structural and thermodynamic analysis of the packing of two α-helices in phage T4 lysozyme. *J. Mol. Biol. 221*, 647–667.

Dao-pin, S., Baase, W.A., & Matthews, B.W. (1990). A mutant T4 lysozyme (Val 131 → Ala) designed to increase thermostability by the reduction of strain within an α-helix. *Proteins Struct. Funct. Genet. 7*, 198–204.

Eriksson, A.E., Baase, W.A., Zhang, X.-J., Heinz, D.W., Blaber, M., Baldwin, E.P., & Matthews, B.W. (1992). The response of a protein structure to cavity-creating mutations and its relationship to the hydrophobic effect. *Science 255*, 178–183.

Faber, H.R. & Matthews, B.W. (1990). A mutant T4 lysozyme displays five different crystal conformations. *Nature 348*, 263–266.

Grütter, M.G., Gray, T.M., Weaver, L.H., Alber, T., Wilson, K., & Matthews, B.W. (1987). Structural studies of mutants of the lysozyme of bacteriophage T4. The temperature sensitive mutant protein Thr 157 → Ile. *J. Mol. Biol. 197*, 315–329.

Grütter, M.G. & Matthews, B.W. (1982). Amino acid substitutions far from the active site of bacteriophage T4 lysozyme reduce catalytic activity and suggest that the C-terminal lobe of the enzyme participates in substrate binding. *J. Mol. Biol. 154*, 525–535.

Hecht, M.H., Sturtevant, J.M., & Sauer, R.T. (1986). Stabilization of λ repressor against thermal denaturation by site-directed Gly → Ala changes in α-helix 3. *Proteins Struct. Funct. Genet. 1*, 43–46.

Heinz, D.W., Baase, W.A., & Matthews, B.W. (1992). Folding and function of a T4 lysozyme containing ten consecutive alanines illustrates the redundancy of information in an amino acid sequence. *Proc. Natl. Acad. Sci. USA* (in press).

Kitamura, S. & Sturtevant, J.M. (1989). A scanning calorimetric study of the thermal denaturation of the lysozyme from phage T4 and the Arg 96 → His mutant form thereof. *Biochemistry 28*, 3788–3792.

Lee, B. & Richards, F.M. (1971). The interpretation of protein structures: Estimation of static accessibility. *J. Mol. Biol. 55*, 379–400.

Lyu, P.C., Liff, M.I., Marky, L.A., & Kallenbach, N.R. (1990). Side-chain contributions to the stability of alpha-helical structure in peptides. *Science 250*, 669–673.

Marqusee, S., Robbins, V.H., & Baldwin, R.L. (1989). Unusually stable helix formation in short alanine-based peptides. *Proc. Natl. Acad. Sci. USA 86*, 5286–5290.

Merutka, G., Lipton, W., Shelonga, W., Park, S.-H., & Stellwagen, E. (1990). Effect of central-residue replacements on the helical stability of a monomeric peptide. *Biochemistry 29*, 7511–7515.

Muchmore, D.C., McIntosh, L.P., Russell, C.B., Anderson, D.E., & Dahlquist, F.W. (1989). Expression and ^{15}N labelling of proteins for proton and nitrogen-15 NMR. *Methods Enzymol. 177*, 44–73.

O'Neil, K.T. & DeGrado, W.F. (1990). A thermodynamic scale for the helix-forming tendencies of the commonly occurring amino acids. *Science 250*, 646–651.

Poteete, A.R., Dao-pin, S., Nicholson, H., & Matthews, B.W. (1991). Second-site revertants of an inactive T4 lysozyme mutant restore activity structuring the active site cleft. *Biochemistry 30*, 1425–1432.

Tronrud, D.E., Ten Eyck, L.F., & Matthews, B.W. (1987). An efficient general-purpose least-squares refinement program for macromolecular structures. *Acta Crystallog. A43*, 489–503.

Weaver, L.H. & Matthews, B.W. (1987). Structure of bacteriophage T4 lysozyme refined at 1.7 Å resolution. *J. Mol. Biol. 193*, 189–199.

Xuong, N.H., Nielsen, C., Hamlin, R., & Anderson, D. (1985). Strategy for data collection from protein crystals using a multiwire counter area detector diffractometer. *J. Appl. Crystallogr. 181*, 342–350.

Zhang, X.-J., Baase, W.A., & Matthews, B.W. (1991). Toward a simplification of the protein folding problem: A stabilizing polyalanine α-helix engineered in T4 lysozyme. *Biochemistry 30*, 2012–2017.